Chem Biol Drug Des 2009; **74:** 43–50

Research Article

doi: 10.1111/j.1747-0285.2009.00833.x

Potent Triazolothione Inhibitor of Heat-Shock Protein-90

Richard I. Feldman*, Bob Mintzer, Daguang Zhu, James M. Wu, Sandra L. Biroc, Shendong Yuan, Kumar Emayan, Zheng Chang, Deborah Chen, Damian O. Arnaiz, Judi Bryant, Xue Snow Ge, Marc Whitlow, Marc Adler, Mark A. Polokoff, Wei-Wei Li, Mike Ferrer, Takashi Sato, Jian-Ming Gu, Jun Shen, Jih-Lie Tseng, Harald Dinter and Brad Buckman

Bayer Healthcare, 2600 Hilltop Drive, Richmond, CA 94804, USA
**Corresponding author: Richard I. Feldman, rick.feldman@bayer.com*

Heat-shock protein-90 is an attractive target for anticancer drugs, as heat-shock protein-90 blockers such as the ansamycin 17-(allylamino)-17-demethoxygeldanamycin greatly reduce the expression of many signaling molecules that are disregulated in cancer cells and are key drivers of tumor growth and metastasis. While 17-(allylamino)-17-demethoxygeldanamycin has shown promise in clinical trials, this compound class has significant template-related drawbacks. In this paper, we describe a new, potent non-ansamycin small-molecule inhibitor of heat-shock protein-90, BX-2819, containing resorcinol and triazolothione rings. Structural studies demonstrate binding of BX-2819 to the ADP/ATP-binding pocket of heat-shock protein-90. The compound blocked expression of heat-shock protein-90 client proteins in cancer cell lines and inhibited cell growth with a potency similar to 17-(allylamino)-17-demethoxygeldanamycin. In a panel of four cancer cell lines, BX-2819 blocked growth with an average IC_{50} value of 32 nM (range of 7–72 nM). Efficacy studies demonstrated that treatment with BX-2819 significantly inhibited the growth of NCI-N87 and HT-29 tumors in nude mice, consistent with pharmacodynamic studies showing inhibition of heat-shock protein-90 client protein expression in tumors for greater than 16 h after dosing. These data support further studies to assess the potential of BX-2819 and related analogs for the treatment of cancer.

Key words: heat shock, Hsp90, inhibitor, small molecule, triazolothione

Abbreviations: 17-AAG, 17-(allylamino)-17-demethoxygeldanamycin; 17-DMAG, 17-(dimethylaminoethylamino)-17-demethoxygeldanamycin; GA, geldanamycin; Hsp90, heat-shock protein-90; Hsp70, cell division cycle 37 homologue; HOP, Hsp organizing protein; Sti1, stress-inducible protein 1; Aha1, activator of Hsp90 ATPase; IGEPAL, octylphenyl-polyethylene glycol.

Received 23 March 2009, revised 9 May 2009 and accepted for publication 11 May 2009

Cancer cells are genetically plastic, exhibiting gene rearrangements, chromosomal losses and gains, and mutations in a large number of genes. This trait underlies the disappointing clinical efficacy often observed for 'targeted' drugs that are directed against a single signaling pathway. A more effective strategy, therefore, may be to simultaneously block a variety of signaling pathways that are key drivers of cancer cell survival and tumor progression. Heat-shock protein-90 (Hsp90) is a molecular chaperone that regulates folding of 'client' proteins with key regulatory roles in growth, survival, differentiation and cancer [for review, see (1–4)]. This involves the formation of complexes of Hsp90 with a variety of interaction proteins, or co-chaperones, such as p23, cell division cycle 37 homologue (Hsp70), Hsp organizing protein, stress-inducible protein-1 and activator of Hsp90 ATPase. Energy from the hydrolysis of ATP drives protein folding and maturation by promoting conformational changes in the Hsp90 molecule that alter the binding of co-chaperone molecules and client proteins.

Several naturally occurring compounds such as the benzoquinone ansamycin, geldanamycin (GA) and radicicol, which selectively bind to the ATP-binding pocket on the *N*-terminal domain of Hsp90, inhibit its function and promote client protein ubiquitylation and degradation through the ubiquitin/proteasome system (2,5). A large number of proteins have been shown to associate with Hsp90 ([a]for an updated list), and Hsp90 inhibitors such as GA appear to be efficient in reducing the expression of signaling proteins including ErbB2, AKT, Raf-1, BRAF, BCR-Abl, Hif-1-alpha and mutant p53, that are important for tumor cell growth or survival. Geldanamycin analogs, such as 17-AAG, block the growth of many tumor cell lines, or promote apoptosis, and have shown promising activity in a variety of cancer models. Phase I and Phase II studies with a number of GA analogs, including 17-AAG and 17-DMAG, demonstrate that Hsp90 inhibition can be achieved in patients with tolerable side-effects and have provided some promising responses (3,6–9). Geldanamycin analogs show significant liabilities, however [e.g., poor solubility, template associated toxicity (benzoquinone moiety), cytochrome P450 interaction and rapid metabolism], warranting the development of new small-molecule Hsp90 inhibitors. In this paper, we describe a potent non-ansamycin small-molecule compound,

BX-2819, whose potency for inhibition of Hsp90 *in vitro* and in cellular assays is as good as 17-AAG. The biological, pharmacological and pharmacodynamic properties of this compound will be discussed. BX-2819 represents a potent new class of Hsp90 inhibitors for evaluation as anti-cancer agents.

Methods and Materials

Cell lines and culture conditions

HT-29 (human colon carcinoma), SKOV3 (human ovarian carcinoma), SKBR3 (human breast carcinoma), NCI-N87 (human gastric carcinoma), and MKN45 (human gastric carcinoma) cell lines were obtained from the American Type Culture Collection (Manassas, VA, USA) and cultured under conditions recommended by the supplier.

Hsp90 competition assays

To assess the affinity of compounds binding to Hsp90, we measured their ability to compete with the binding of a fluorescent analog of GA (GM-Bodipy) (10) to Hsp90, using fluorescence polarization. As described previously (11), displacement of bound GM-Bodipy from the *N*-terminal ATP-binding site of Hsp90α results in a decrease in fluorescence polarization values (expressed in mP). Fluorescence measurements were made with a Perkin Elmer Envision instrument in black 384-well Perkin Elmer Optiplates (Perkin Elmer, Waltham, MA, USA). The final binding mixture contained 100 nM Hsp90α (Stressgen Bioreagents, Ann Arbor, MI, USA), 100 nM GM-Bodipy, 20 mM HEPES, pH 7.4, 50 mM KCl, 1 mM DTT, 5 mM $MgCl_2$, 20 mM Na_2MoO_4, 0.01% IGEPAL-CA630 and 0.1 mg/mL bovine gamma globulin. Test compounds and controls were delivered in DMSO, resulting in a final DMSO concentration of 2.5%. Following addition of assay components, plates were centrifuged 1 min at 1000 rpm (to ensure complete mixing of assay components) sealed, incubated overnight (16 h) at room temperature, and finally read.

Hsp90 crystallization and X-ray analysis

The purified *N*-terminal domain of Hsp90 (228 amino acids) was obtained from CRELUX GmbH (Martinsried, Germany). Crystallography of Hsp90:BX-2819 complexes was performed and X-ray data collected and analyzed as described by Stebbins *et al.* (12).

ErbB2/Her2 expression assay

We measured expression of ErbB2 in cultured SKBR3 cells as previously described (10), with minor modifications. SKBR3 cells were seeded in black, clear-bottom 96-well plates (Corning, 3603; Lowell, MA, USA) [5000 cells per well in 100 μL DME:F12 (1:1), 5% heat-inactivated FBS, 2 mM glutamine]. After 48 h incubation at 37°C in 5% CO_2, we added test compounds, dissolved in DMSO, to yield a final DMSO concentration of 0.1%. Following treatment with test compounds for 16 h, we washed cells twice with ice-cold Tris-buffered saline with 0.1% Tween 20 (TBST) and fixed them by addition of 100 μL methanol (−20°C), followed by an incubation at 4°C for 10 min. After washing twice with TBST, we blocked the plates for 1 h at room temperature with SuperBlock (Pierce Chemicals, Rockford, IL, USA), followed by addition of 100 μL/well of anti-ErbB2 antibody [SC-284, (Santa Cruz Biotechnology, Santa Cruz, CA, USA)], diluted 1:200 in fresh SuperBlock. After incubation overnight at 4°C, we washed twice with TBST, and treated 1 h at room temperature with anti-rabbit HRP-conjugated antibody (Sigma, St Louis, MO, USA; A0545) (100 μL/well), diluted 1:1000 in SuperBlock. After removing unbound antibody by washing three times with TBST, we added SuperSignal chemiluminescent substrate (Pierce Chemicals) (100 μL/well) and after 10 min, we read the plates on a Packard TopCount.

Immunoblotting and ELISA assays

After treating cells (roughly 80% confluent) as described in the figures, we washed them once with phosphate buffered saline and then lysed them with mammalian protein extraction (MPER) reagent (Pierce Chemicals), supplemented with protease and phosphatase inhibitors [Halt protease inhibitor cocktail (Pierce Chemicals), 1-mM sodium fluoride and 1-mM sodium orthovanadate]. For analysis of lysates by Western blotting, we used antibodies against Hsp70 from Stressgen, ErbB2, C-Met and Raf1 from Santa Cruz Biotechnology, and Phospho-AKT from Cell Signaling Technology (Danvers, MA, USA). For analysis of protein levels by ELISA, we performed measurements using kits for ErbB2 (Calbiochem, La Jolla, CA, USA) or Hsp70 (R&D Systems Inc., Minneapolis, MN, USA), according to the manufacturer's instructions.

Growth assays

We seeded cells at low density (1500–3000 cells per well in 96-well plates) in a volume of 0.1 mL and after an overnight incubation, added compounds (10 μL/well), dissolved in 1% DMSO/growth medium. After 72 h of treatment, we determined the number of viable cells using the metabolic dye, WST-1 (Roche Applied Science, Indianapolis, IN, USA), measuring the absorbance of WST-1 at 450 nm.

Animal tumor models

Athymic (nu/nu) female mice (Simonsen, Gilroy CA, USA), 6–8 weeks of age, were used in all experiments. We induced HT-29, SKOV3, or NCI-N87 tumors by s.c. implantation of tumor fragments harvested from donor mice. After 2–4 weeks, mice with tumors of 200–500 mm^3 were sorted into groups of 10. Transponders (BMDS, Seaford, DE, USA) were implanted s.c. to facilitate identification of individual mice. We dosed animals with BX-2819, dissolved in Tween 80/EtOH/H_2O (3%/2%/95%), i.p., twice weekly (q3-4d) in a volume of 250 μL/mouse. To estimate tumor volume, we made caliper measurements of two perpendicular tumor diameters and calculated the tumor volume using the formula $(L \times W \times W)/2 = V$, where L is longest diameter, W is shortest diameter and V equals the volume (in mm^3). The chronic BX-2819 treatments resulted in minimal body weight loss and no animal deaths. For the pharmacodynamic study, we gave a cohort of tumor-bearing mice a single application of BX-2819 at 100 mg/kg and euthanized groups of three mice at various times thereafter. All animal procedures followed the National and International guidelines for humane treatment of animals and were approved by our Institutional Animal Care and Use Committee. For statistical analyses, we performed the Kruskal–Wallis test and the Wilcoxon non-parametric

(Mann–Whitney *U*) analysis using the computer program JMP 5.0 (SAS Institute, Inc., Cary, NC, USA). A p-value of <0.05 was considered significant.

Quantification of BX-2819 in plasma and tumor

For pharmacokinetic studies, we collected blood into Microtainer blood collection tubes (BD Biosciences, Franklin Lakes, NJ, USA) and prepared plasma by centrifugation at 5000 × *g* for 10 min. To determine compound levels in tumor tissue, we weighed excised tumors, added a threefold excess of 0.1% Triton X-100 in water, and. homogenized the tissue for 2 min at medium speed in an Omnimixer (TH115-PCR-D; Omni International, Marietta, GA, USA) with disposable probes. We transferred ~1.5 mL of homogenate to a 2-ml tube containing ceramic beads and garnet sand, which was shaken vigorously using a Savant FastPrep apparatus (Qbiogene Inc, Carlsbad, CA, USA). Compound levels in a 50-μL aliquot of the extract were determined by LC/MS/MS as follows. Proteins in the sample were precipitated by addition of fourfold excess (200 μL) of acetonitrile. The sample was centrifuged and a 5-uL aliquot of the supernatant was analyzed on a Varian Polaris C18-A (Varian Polaris, Palo Alto, CA, USA), 3 μm, 2×50 mm HPLC column at a flow rate of 0.2 mL/min using a gradient of 10–80% A (water + 0.1% formic acid) to B (acetonitrile + 0.1% formic acid). Tandem mass spectrometer (MS/MS) analysis was performed on an ABI 3000 instrument (Applied Biosystems, Foster City, CA, USA). The compound concentration in tumor lysates is expressed as μg/g, taking into account the original 1:4 dilution in homogenization fluid.

Results and Discussion

Identification of novel triazolothione compounds that block Hsp90 activity in vitro *and in cells*

We performed high throughput screening to identify Hsp90 inhibitors that compete with the binding of GA, labeled with the fluorescent tag bodipy (GM-Bodipy). The resorcinol analog **1** (Figure 1) was among the Hsp90 inhibitors we identified, which we optimized through parallel paths on its two aryl rings, as outlined in Figure 1. Unsubstituted phenyl ring analog **2** was nearly equipotent with the starting naphthyl analog **1**, thus we tested the potency of a large number of aryl substituted compounds. Ethyl carbamate **3** was among the best we examined. Among the resorcinol ring substitutions we tested, the ethyl analog (**4**) increased potency modestly, whereas the isopropyl analog (**5**) was found to be the optimum substitution at this position. Combination of these optimized substituents provided BX-2819, whose synthesis is outlined in Figure 2.

BX-2819 binds potently to Hsp90, displaying an IC_{50} of 41 nM for inhibition of GM-Bodipy binding, which was lower than either 17-AAG (IC_{50} = 350 nM) or radicicol (IC_{50} = 87 nM) (Figure 3A). BX-2819 is distinct from ansamycins, such as 17-AAG, but shares some similarity to radicicol (13,14), in that it contains a dihydroxyphenyl resorcinol moiety. BX-2819 also has structural similarity to a series of compounds described in the literature that contain resorcinol and pyrazole/isoxazole amide rings (15) which have been optimized to yield potent Hsp90 inhibitors, such as NVP-AUY922 (2,16). A key characteristic of Hsp90 inhibitors, such as 17-AAG, is their ability to promote the degradation of Hsp90 client proteins such as ErbB2/Her2 in cancer cells. Therefore, we measured the effect of BX-2819 on surface expression of ErbB2 in SKBR3 ovarian cancer cells after overnight treatment. As shown in Figure 3B, BX-2819 potently blocked the expression of ErbB2 with an IC_{50} of 23 nM. 17-AAG or radicicol displayed roughly fivefold less potent activity in this assay. BX-2819 also potently blocked ErbB2 expression in HT-29 colon cancer cells (Figure 3C) and OVCAR3 ovarian cancer cells (not shown), with a potency similar to 17-AAG. Furthermore, BX-2819 strongly stimulated the expression of Hsp70, which is another well-studied hallmark of Hsp90 inhibition in cells, resulting from the release of the transcription factor heat-shock factor-1 from its binding site of Hsp90 (17). Taken together, these data indicate that BX-2819 binds to Hsp90 in cells with high affinity and in a manner competitive with GA, blocking Hsp90 function and effectively promoting the degradation of an Hsp90 client protein.

Structure of BX-2819 bound to Hsp90

To determine the mode of BX-2819 binding to Hsp90, we solved the crystal structure of the compound in complex with the ATP-

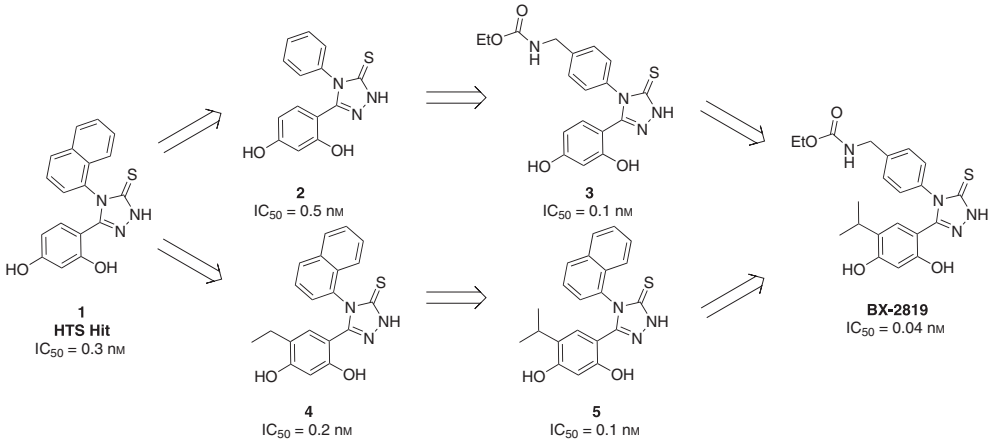

Figure 1: Lead optimization yielding BX-2819.

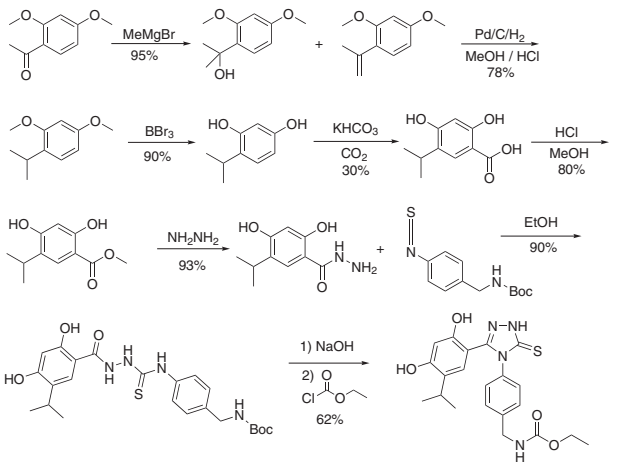

Figure 2: Scheme for synthesis of BX-2819.

binding domain of Hsp90. The structure (Figure 4A) indicates that BX-2819 binds in the ATP/ADP-binding pocket of Hsp90 in a manner similar to several other inhibitors that include a resorcinol ring (12,18–20).

Figure 4B shows the binding of BX-2819 to Hsp90 relative to the binding of ADP. The resorcinol and triazolothione rings of BX-2819 fill the same space occupied by the purine ring of bound ADP (pdb code 1BYQ), whereas the phenyl moiety extends into the ribose-binding site, and the carbamate mimics ADP's α-phosphate. Previous work has shown that GA also binds inside this same cleft [(12), pdb code 1YET], consistent with the competition of BX-2819 and GA for binding to Hsp90.

At the base of the binding cleft, the resorcinol ring of BX-2819 forms two hydrogen bonds (H-bonds) through its two hydroxyl groups. One hydroxyl interacts with carboxylic acid of Asp93 (2.7 Å). A similar H-bond (Figure 4B) is formed by the amine on ADP (2.9 Å). The second hydroxyl on the phenol ring forms an H-bond to a conserved water (2.7 Å) that is found in nearly all the Hsp90 structures that have been reported. The isopropyl substituent on the resorcinol ring of BX-2819 is buried in a small hydrophobic pocket that is lined by the side chains of Ile107 (3.3 Å), Phe138 (4.0 Å) and Val150 (4.1 Å). The isopropyl also makes an intramolecular contact with the second phenyl ring in the inhibitor.

The triazolothione ring of BX-2819 forms two H-bonds: a water-mediated H-bond to the side chain of Thr184 (3.0 Å) and a second direct H-bond to the carbonyl of Gly97 (3.0 Å). Similar interactions were also seen in homologous inhibitors that contain a pyrazole ring (12,19,20). The amide from the carbamate of BX-2819 donates an H-bond to the side chain of Asn51 (3.1 Å) and the carbamate carbonyl accepts an H-bond from the amide of Phe138 (3.0 Å). A similar H-bond is formed by one of the α-phosphate oxygens in ADP (3.0 Å) and by the carbonyl in GA (2.8 Å).

It should be noted that Hsp90 and BX-2819 co-crystallized into the $P2_12_12$ space group and there were two copies of the protein in the asymmetric unit. The carbamate group adopted a different conformation in each subunit in response to changes in the protein conformation involving the sequential four and five helixes (residues 101–124). Similar heterogeneity in the protein conformation had been reported for this crystal form of Hsp90 (20,21), although the alterations in protein conformation did not significantly perturb the inhibitors. There is no direct experimental evidence that indicates which of the two inhibitor conformations corresponds to the solution state of the Hsp90/BX-2819 complex. However, both the inhibitor and the protein structure shown in Figure 4 are similar to the binding of ADP and GA in Hsp90 (12,22). The second conformation has an unusual H-bond between the carbamate and the amide of Ile110, which we have not seen in other Hsp90 structures.

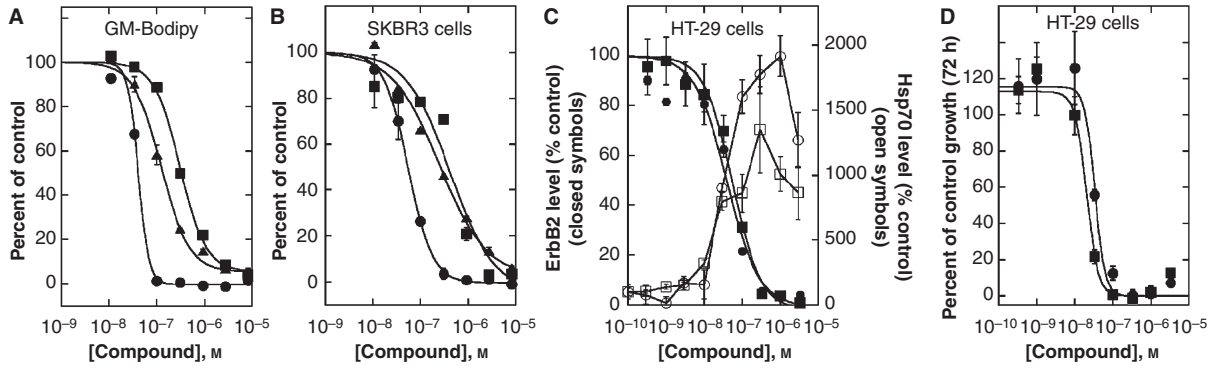

Figure 3: Inhibitor binding to Hsp 90, effect on Hsp 90 client proteins in cells and inhibition of tumor cell growth. (A) The binding of BX-2819 to recombinant Hsp 90 was determined by competition with Bodipy-labeled-geldanamycin as described under 'Materials and Methods.' Representative curves are shown for BX-2819 (solid circles) [IC_{50} = 41 ± 5 nM (n = 6)]; 17-AAG (solid squares) [IC_{50} = 350 ± 120 nM (n = 28)]; and radicicol (solid triangles) [IC_{50} = 87 ± 47 nM (n = 16)]. (B) The inhibition of Hsp 90 function in cells was assessed by measuring expression levels of the Hsp 90 client protein ErbB2 in SKBR3 cells after overnight treatment with compounds. Representative curves are shown for BX-2819 (solid circles) (IC_{50} = 23 ± 8 nM (n = 5)]; 17-AAG (solid squares) [IC_{50} = 130 ± 70 nM (n = 14)]; and radicicol (solid triangles) (IC_{50} = 130 ± 100 nM (n = 9)]. (C) The effect of BX-2819 (circles) and 17-AAG (squares) on ErbB2 (solid symbols) and Hsp 70 (open symbols) protein expression in HT-29 cancer cells after overnight treatment with compounds. ErbB2 and Hsp 70 levels were determined by ELISA. (D) Effect of BX-2819 (circles) and 17-AAG (squares) on the growth of HT-29 cancer cells.

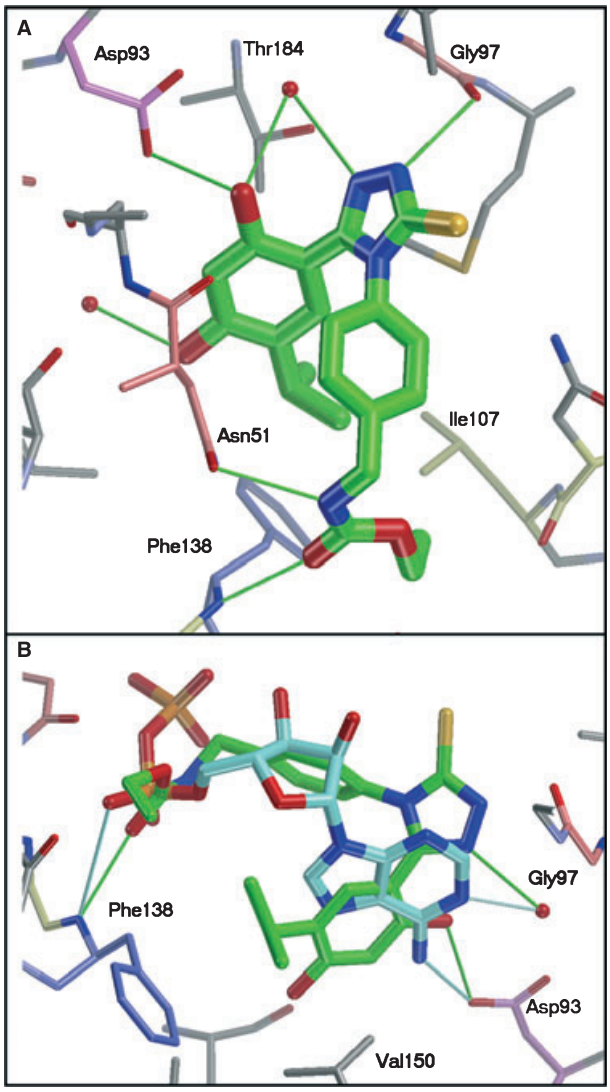

Figure 4: Structure of BX-2819 bound to Hsp 90 determined by X-ray diffraction. BX-2819 bound to Hsp 90 is shown in panel A, with indicated hydrogen bonds to Hsp 90 residues or bound water (pdb code 4HHU). Panel B shows a superimposition of BX-2819 (green) with ADP (light blue) bound to Hsp 90.

BX-2819 blocks Hsp90 client protein expression and inhibits growth of cancer cell lines

To further examine the effect of BX-2819 on signaling pathways regulated by Hsp90, we profiled BX-2819, and the comparator compound, 17-AAG, on expression of a number of Hsp90 client proteins in NCI-N87 and MKN-45 gastric carcinoma cancer cells. As shown in Figure 5, treatment of both cells with BX-2819 reduced expression of ErbB2, Raf1 and c-Met protein to levels undetectable by Western blotting, with the half-maximal effect occurring between 10 and 100 nM. Formation of phospho-AKT was also strongly inhibited, possibly through an inhibition of AKT expression or loss of signaling from receptors such as ErbB2 or C-Met. As is seen with 17-AAG, and other classes of Hsp90 inhibitors studied, BX-2819 promoted an increase in Hsp70

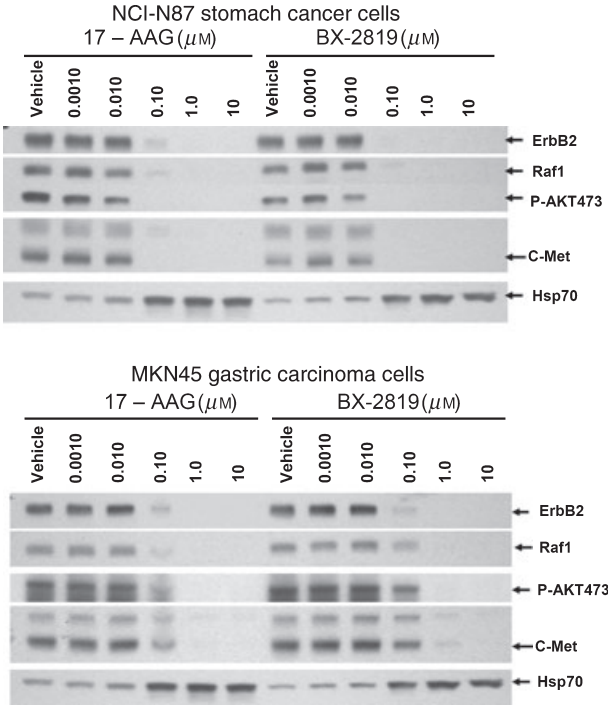

Figure 5: BX-2819 inhibits expression of Hsp 90 client proteins in NCI-N87 stomach cancer and MKN45 gastric carcinoma cells. Cells were incubated overnight with vehicle, or various concentrations of 17-AAG or BX-2819, and client protein expression was determined by Western blotting as described under 'Materials and Methods.'

protein levels with an IC_{50} value similar to those for inhibition of Hsp90 client protein expression. These data further demonstrate that BX-2819 blocks the function of Hsp90 in cancer cells with a potency as great as 17-AAG.

Although a long list of proteins appears to associate with Hsp90, the effect of Hsp90 on their expression can vary widely. Expression of ErbB2 and Raf1 have been found to be particularly sensitive to downregulation by 17-AAG and other Hsp90 inhibitors. NCI-N87 and MKN45 cells express high levels of C-Met. For MKN45 cells, growth in cell culture depends on ligand-induced activation of C-Met (23), and small-molecule inhibitors of C-Met promote regression of MKN45 tumors xenografts in nude mice (24). BX-2819 effectively blocked C-Met expression in MKN45 and NCI-N87 cells (Figure 5) with an $IC_{50} \sim 50$ nM, which is only slightly less potent than compound-mediated inhibition of ErbB2 expression, and similar to the potency of Raf1 downregulation ($IC_{50} = 100$ nM). These data suggest that tumors dependent on C-Met for growth, such as gastric carcinomas or liver cancers, may be a good indication for treatment with Hsp90 inhibitors.

To assess whether BX-2819 is an effective inhibitor of tumor cell growth, we determined its effect on the proliferation of SKBR3, SKOV3, MKN45, and NCI-N87 cells (Table 1). BX-2819 potently blocked the growth of all four cell lines (average $IC_{50} = 32$ nM), with IC_{50} values ranging from 7 nM (NCI-N87 cells) to 72 nM

Table 1: Inhibition of tumor cell growth by Hsp90 inhibitors

Cell line	BX-2819 [nM; IC_{50} (*n*)]	17-AAG [nM; IC_{50} (*n*)]
SKBR3	14 ± 1 (4)	11 ± 3 (4)
SKOV3	36 ± 6 (4)	28 ± 3 (4)
MKN-45	72 ± 10 (4)	62 ± 9 (4)
NCI-N87	7 ± 1 (4)	5 ± 2 (4)

Table 2: Pharmacokinetic parameters of BX 2819 in rat

Dose (mg/kg)	Route	$t_{1/2}$ (h)	AUC_{inf} (μg h/mL)	CL (mL/min/kg)	V_{ss} (L/kg)
2	iv	0.8	0.23	159	4.5

Data are from three rats, dosed using 10% DMSO/90% PEG300 as the vehicle.

(MKN45 cells). 17-AAG exhibited very similar growth inhibitory potency for our tumor cell panel (average IC_{50} = 27 nM) (Table 1). BX-2819 displayed no apparent toxicity on non-dividing HepG2 cells or normal renal proximal tubular epithelial cells (RPTEC) in culture, at concentrations up to 100 μM, as assessed by measuring ATP levels (data not shown). Ansamycins such as 17-AAG have been reported to exhibit a cytotoxic effect on cells, which has been attributed to the benzoquinone moiety on the molecule. Our data indicate that potent non-ansamycin Hsp90 inhibitors, such as BX-2819, can be equally effective at blocking growth of tumor cells in culture without such toxicities.

BX-2819 promotes degradation of ErbB2 in tumors

To assess the ability of BX-2819 to block Hsp90 in tumors, we injected BX-2819 (100 mg/kg) i.p. into mice bearing subcutaneous NCI-N87 or SKOV3 tumors. As shown in Figure 6, the compound greatly suppressed tumor ErbB2 expression for the duration of the experiment (16 h), while promoting a 5- to 10-fold increase in Hsp70 expression, consistent with the *in vitro* effects of the compound on tumor cells. These data indicate that BX-2819 can reach NCI-N87 and SKOV3 tumors and effectively suppress Hsp90 client protein expression for a prolonged period of time. To assess the metabolic stability of BX-2819, we incubated the compound with liver microsomes (including a NADPH/NADH-regenerating system). After 1 h of incubation, 74%, 66%, 79% and 80% of intact BX-2819 remained using rat, dog, human, or mouse microsomes, respectively. While these studies show that BX-2819 is relatively stable metabolically and displays a long duration of action in tumors, pharmacokinetic studies of BX-2819 in rats (Table 2) indicate that BX-2819 has a relatively short serum half life ($t_{1/2}$ = 0.8 h) and high clearance (CL = 159 mL/min/kg) and a high volume of distribution (V_{ss} = 4.5 L).

A number of Hsp90 inhibitors, such as 17-AAG and purine-scaffold inhibitors, clear relatively rapidly from plasma, but accumulate into tumors and show long-lasting effects on Hsp90 client protein expression (25–27). To determine whether BX-2819 shows a similar behavior, we dosed mice bearing SKBR3 or NCI-N87 tumors with BX-2819 (100 mg/kg i.p.), and determined compound levels in the tumors and plasma after various times. As shown in Figure 7, by the first time point of 3 h, BX-2819 levels in SKBR3 and NCI-N87 tumors were five- to sixfold higher than that found in the plasma. By 10 h, the tumor to plasma ratio was roughly 100, and for SKOV3 tumors, reached 350 by 50 h after dosing (Figure 7). Compound levels in tumors remained >1 μg/g (corresponding to $\sim$2 μM) for at least 20 h. These data suggest that the rapid elimination of BX-2819 from plasma may possibly be driven by compound binding to the abundant levels of Hsp90 present in tissues and tumors. These kinetics are seemingly consistent with the long-lasting suppression of ErbB2 expression in SKOV3 and NCI-N87 tumors we observed (>16 h) (Figure 6). However, it should be noted that given the high level of expression of Hsp90 reported in normal and tumor tissues (1–2% of cellular protein, corresponding to $\sim$100 μM), the level of BX-2819 accumulating in tumors could bind only a small percentage of the total Hsp90 pool. As suggested by others (28,29), this fact may indicate that only a small percentage of Hsp90 mole-

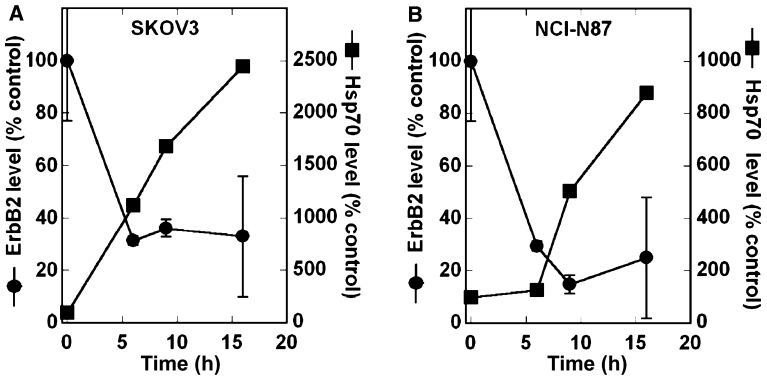

Figure 6: BX-2819 blocks Hsp 90 function in tumors. BX-2819 (100mg/kg) or vehicle were administered once i.p. to nude mice bearing s.c. NCI-N87 or SKOV3 tumors. Groups of five mice were euthanized at 3 h after vehicle dosing, or 6, 9, or 16 h after BX-2819 dosing and the SKOV-3 (A) or NCI-N87 (B) tumors were analyzed for expression of ErbB2 or Hsp 70, by Western Blotting, as described under 'Materials and Methods.' Solid squares represent relative Hsp 70 levels, and solid circles represent ErbB2 levels. Each value (n = 5) represents the average per cent increase or decrease over the vehicle control (3 h) ± SEM.

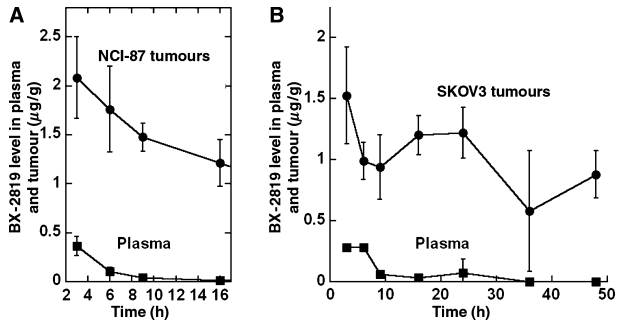

Figure 7: Pharmacokinetics of BX-2819 in tumor bearing mice. Mice bearing s.c. NCI-N87 or SKOV3 tumors were dosed i.p. with BX-2819 (100 mg/kg), and at the times indicated, groups of three animals were euthanized. Compound levels were determined in the plasma and tumors as described under 'Materials and Methods,' and represent the average of three determinations ± SEM.

cules expressed in cells form the necessary complexes that function in client protein regulation and bind inhibitors such as BX-2819 with high affinity.

BX-2819 blocks the growth of tumors in animals

We evaluated the efficacy of BX-2819 in NCI-N87 gastric carcinoma and HT-29 colon cancer xenograft models in nude mice. Based on the long-lasting duration of action we observed for BX-2819, discussed above, we administered the compound twice weekly i.p., at a dose of 100 mg/kg. As shown in Figure 8, this treatment promoted a significant decrease in tumor growth and final tumor burden in both HT-29 and NCI-N87 models. BX-2819 showed particularly good efficacy in the NCI-N87 model, in accordance with its higher sensitivity *in vitro*. The ability of twice weekly dosing of BX-2819 to inhibit tumor growth is consistent with the long-lasting suppression of client protein expression we observed in the pharmacodynamic studies discussed above, and the compound's ability to accumulate into tumors. While there was transient body weight loss immediately after the intermittent dosing, there were no animal deaths in the studies. These data indicate that BX-2819 has potential as a therapeutic agent in a variety of cancers.

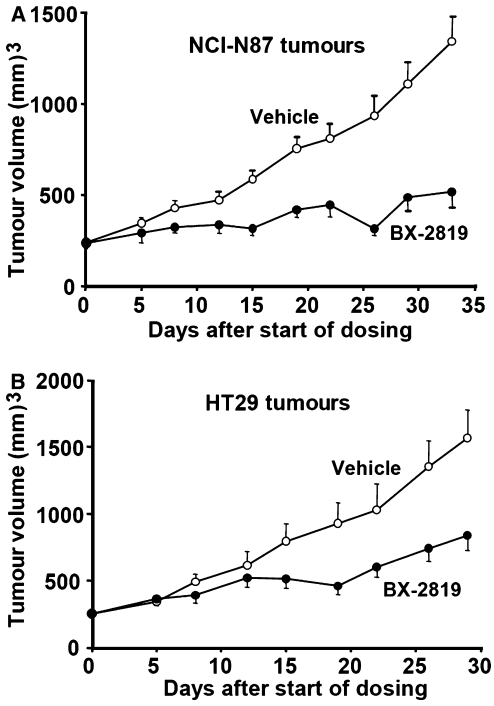

Figure 8: BX-2819 blocks the growth of tumors in nude mice. Vehicle or BX-2819 was administered to nude mice bearing s.c. NCI-N87 or SKOV3 tumors by i.p. injection. At the times indicated, animals (10 animals per treatment group) were sacrificed and tumors were measured as described under 'Materials and Methods.'

In summary, we have described a potent new non-ansamycin inhibitor of Hsp90, BX-2819, which binds to Hsp90 as potently as ansamycins such as 17-AAG, which are currently being evaluated in the clinic as anticancer drugs. BX-2819 does not contain the potentially toxic benzoquinone moiety, and showed no apparent toxicity in non-dividing cells. Significantly, BX-2819 exhibited potent inhibition of Hsp90 in various cancer cell lines, suppressed Hsp90 client protein expression in tumor xenografts for over 16 h after i.p. administration, and effectively inhibited tumor growth in several animal models. These studies support further evaluation of BX-2819, or other triazolothione analogs, as anticancer drugs.

References

1. Pearl L.H., Prodromou C., Workman P. (2008) The Hsp90 molecular chaperone: an open and shut case for treatment. Biochem J;410:439–453.
2. Messaoudi S., Peyrat J.F., Brion J.D., Alami M. (2008) Recent advances in Hsp90 inhibitors as antitumor agents. Anticancer Agents Med Chem;8:761–782.
3. Solit D.B., Chiosis G. (2008) Development and application of Hsp90 inhibitors. Drug Discov Today;13:38–43.
4. Burrows F., Zhang H., Kamal A. (2004) Hsp90 activation and cell cycle regulation. Cell Cycle;3:1530–1536.
5. Whitesell L., Mimnaugh E.G., De Costa B., Myers C.E., Neckers L.M. (1994) Inhibition of heat shock protein HSP90-pp60v-src heteroprotein complex formation by benzoquinone ansamycins: essential role for stress proteins in oncogenic transformation. Proc Natl Acad Sci U S A;91:8324–8328.
6. Sharp S., Workman P. (2006) Inhibitors of the HSP90 molecular chaperone: current status. Adv Cancer Res;95:323–348.
7. Modi S., Stopeck A.T., Gordon M.S., Mendelson D., Solit D.B., Bagatell R., Ma W., Wheler J., Rosen N., Norton L., Cropp G.F., Johnson R.G., Hannah A.L., Hudis C.A. (2007) Combination of trastuzumab and tanespimycin (17-AAG, KOS-953) is safe and active in trastuzumab-refractory HER-2 overexpressing breast cancer: a phase I dose-escalation study. J Clin Oncol;25:5410–5417.
8. Pacey S., Banerji U., Judson I., Workman P. (2006) Hsp90 inhibitors in the clinic. Handb Exp Pharmacol;172:331–358.
9. Weigel B.J., Blaney S.M., Reid J.M., Safgren S.L., Bagatell R., Kersey J., Neglia J.P., Ivy S.P., Ingle A.M., Whitesell L., Gilbert-

son R.J., Krailo M., Ames M., Adamson P.C. (2007) A phase I study of 17-allylaminogeldanamycin in relapsed/refractory pediatric patients with solid tumors: a Children's Oncology Group study. Clin Cancer Res;13:1789–1793.
10. Llauger L., He H., Kim J., Aguirre J., Rosen N., Peters U., Davies P., Chiosis G. (2005) Evaluation of 8-arylsulfanyl, 8-arylsulfoxyl, and 8-arylsulfonyl adenine derivatives as inhibitors of the heat shock protein 90. J Med Chem;48:2892–2905.
11. Llauger-Bufi L., Felts S.J., Huezo H., Rosen N., Chiosis G. (2003) Synthesis of novel fluorescent probes for the molecular chaperone Hsp90. Bioorg Med Chem Lett;13:3975–3978.
12. Stebbins C.E., Russo A.A., Schneider C., Rosen N., Hartl F.U., Pavletich N.P. (1997) Crystal structure of an Hsp90-geldanamycin complex: targeting of a protein chaperone by an antitumor agent. Cell;89:239–250.
13. Schulte T.W., Akinaga S., Soga S., Sullivan W., Stensgard B., Toft D., Neckers L.M. (1998) Antibiotic radicicol binds to the N-terminal domain of Hsp90 and shares important biologic activities with geldanamycin. Cell Stress Chaperones;3:100–108.
14. Agatsuma T., Ogawa H., Akasaka K., Asai A., Yamashita Y., Mizukami T., Akinaga S., Saitoh Y. (2002) Halohydrin and oxime derivatives of radicicol: synthesis and antitumor activities. Bioorg Med Chem;10:3445–3454.
15. Cheung K.M., Matthews T.P., James K., Rowlands M.G., Boxall K.J., Sharp S.Y., Maloney A., Roe S.M., Prodromou C., Pearl L.H., Aherne G.W., McDonald E., Workman P. (2005) The identification, synthesis, protein crystal structure and in vitro biochemical evaluation of a new 3,4-diarylpyrazole class of Hsp90 inhibitors. Bioorg Med Chem Lett;15:3338–3343.
16. Brough P.A., Aherne W., Barril X., Borgognoni J., Boxall K., Cansfield J.E., Cheung K.M. *et al.* (2008) 4,5-diarylisoxazole Hsp90 chaperone inhibitors: potential therapeutic agents for the treatment of cancer. J Med Chem;51:196–218.
17. Morimoto R.I. (1998) Regulation of the heat shock transcriptional response: cross talk between a family of heat shock factors, molecular chaperones, and negative regulators. Genes Dev;12:3788–3796.
18. Roe S.M., Prodromou C., O'Brien R., Ladbury J.E., Piper P.W., Pearl L.H. (1999) Structural basis for inhibition of the Hsp90 molecular chaperone by the antitumor antibiotics radicicol and geldanamycin. J Med Chem;42:260–266.
19. Kreusch A., Han S., Brinker A., Zhou V., Choi H.S., He Y., Lesley S.A., Caldwell J., Gu X.J. (2005) Crystal structures of human HSP90alpha-complexed with dihydroxyphenylpyrazoles. Bioorg Med Chem Lett;15:1475–1478.
20. Dymock B.W., Barril X., Brough P.A., Cansfield J.E., Massey A., McDonald E., Hubbard R.E., Surgenor A., Roughley S.D., Webb P., Workman P., Wright L., Drysdale M.J. (2005) Novel, potent small-molecule inhibitors of the molecular chaperone Hsp90 discovered through structure-based design. J Med Chem;48:4212–4215.
21. Barril X., Brough P., Drysdale M., Hubbard R.E., Massey A., Surgenor A., Wright L. (2005) Structure-based discovery of a new class of Hsp90 inhibitors. Bioorg Med Chem Lett;15:5187–5191.
22. Obermann W.M., Sondermann H., Russo A.A., Pavletich N.P., Hartl F.U. (1998) In vivo function of Hsp90 is dependent on ATP binding and ATP hydrolysis. J Cell Biol;143:901–910.
23. Shinomiya N., Gao C.F., Xie Q., Gustafson M., Waters D.J., Zhang Y.W., Vande Woude G.F. (2004) RNA interference reveals that ligand-independent met activity is required for tumor cell signaling and survival. Cancer Res;64:7962–7970.
24. Bellon S.F., Kaplan-Lefko P., Yang Y., Zhang Y., Moriguchi J., Rex K., Johnson C.W. *et al.* (2008) c-Met inhibitors with novel binding mode show activity against several hereditary papillary renal cell carcinoma-related mutations. J Biol Chem;283:2675–2683.
25. He H., Zatorska D., Kim J., Aguirre J., Llauger L., She Y., Wu N., Immormino R.M., Gewirth D.T., Chiosis G. (2006) Identification of potent water soluble purine-scaffold inhibitors of the heat shock protein 90. J Med Chem;49:381–390.
26. Eiseman J.L., Lan J., Lagattuta T.F., Hamburger D.R., Joseph E., Covey J.M., Egorin M.J. (2005) Pharmacokinetics and pharmacodynamics of 17-demethoxy 17-[[(2-dimethylamino)ethyl]amino]geldanamycin (17DMAG, NSC 707545) in C.B-17 SCID mice bearing MDA-MB-231 human breast cancer xenografts. Cancer Chemother Pharmacol;55:21–32.
27. Banerji U., Walton M., Raynaud F., Grimshaw R., Kelland L., Valenti M., Judson I., Workman P. (2005) Pharmacokinetic-pharmacodynamic relationships for the heat shock protein 90 molecular chaperone inhibitor 17-allylamino, 17-demethoxygeldanamycin in human ovarian cancer xenograft models. Clin Cancer Res;11:7023–7032.
28. Chiosis G., Neckers L. (2006) Tumor selectivity of Hsp90 inhibitors: the explanation remains elusive. ACS Chem Biol;1:279–284.
29. Kamal A., Thao L., Sensintaffar J., Zhang L., Boehm M.F., Fritz L.C., Burrows F.J. (2003) A high-affinity conformation of Hsp90 confers tumour selectivity on Hsp90 inhibitors. Nature;425:407–410.

Note

[a]http://www.picard.ch/downloads/Hsp90interactors.pdf.